Genetic Segregation of Spontaneous Erosive Arthritis and Generalized Autoimmune Disease in the BXD2 Recombinant Inbred Strain of Mice

J. D. Mountz*†, P. Yang*, Q. Wu*, J. Zhou*, A. Tousson‡, A. Fitzgerald*, J. Allen*, X. Wang*, S. Cartner§, W. E. Grizzle§, N. Yi¶, L. Lu**, R. W. Williams** & H.-C. Hsu*

*Department of Medicine, Division of Clinical Immunology and Rheumatology, the University of Alabama at Birmingham; †Veterans Administration Medical Center; ‡Department of Cell Biology, the University of Alabama at Birmingham; §Department of Comparative Medicine; ¶Section of Statistical Genetics, Department of Statistics, the University of Alabama at Birmingham, Birmingham, AL; and **Center for Neuroscience and Department of Anatomy and Neurobiology, University of Tennessee, Memphis, TN, USA

Received 18 October 2004; Accepted in revised form 22 November 2004

Correspondence to: Dr Hui-Chen Hsu, PhD, 701 19th Street South, LHRB 473, The University of Alabama at Birmingham, Birmingham, AL 35294, USA. E-mail: huichen.hsu@ccc.uab.edu

Abstract

The BXD2 strain of mice is one of approximately 80 BXD recombinant inbred (RI) mouse strains derived from an intercross between C57BL/6J (B6) and DBA/2J (D2) strains. We have discovered that adult BXD2 mice spontaneously develop generalized autoimmune disease, including glomerulonephritis (GN), increased serum titres of rheumatoid factor (RF) and anti-DNA antibody, and a spontaneous erosive arthritis characterized by mononuclear cell infiltration, synovial hyperplasia, and bone and cartilage erosion. The features of lupus and arthritis developed by the BXD2 mice segregate in F2 mice generated by crossing BXD2 mice with the parental B6 and D2 strains. Genetic linkage analysis of the serum levels of anti-DNA and RF by using the BXD RI strains shows that the serum titers of anti-DNA and RF were influenced by a genetic locus on mouse chromosome (Chr) 2 near the marker *D2Mit412* (78 cM, 163 Mb) and on Chr 4 near *D4Mit146* (53.6 cM, 109 Mb), respectively. Both loci are close to the B-cell hyperactivity, lupus or GN susceptibility loci that have been identified previously. The results of our study suggest that the BXD2 strain of mice is a novel model for complex autoimmune disease that will be useful in identifying the mechanisms critical for the immunopathogenesis and genetic segregation of lupus and erosive arthritis.

Introduction

Both rheumatoid arthritis (RA) and systemic lupus erythematosus (SLE or lupus) are complex, multigenetic diseases that are associated with autoantibody production and immune complex deposition. The features of these diseases manifest themselves in a complex environment of generalized autoimmunity and it has been difficult to dissect the factors that drive the course of the disease from those that determine the magnitude of the responses and those that are secondary effects of disease processes.

The mouse models that are available currently either do not develop arthritis or have a single-gene defect that limits their application to dissecting disease cause and effect. Several multigenetic mouse models of generalized autoimmune disease are available, including NZB/W, NZM2410 and (MRL-Fas^{lpr} × B6-Fas^{lpr})F_2 mice, but these mice do not develop arthritis spontaneously although it can be induced in a certain percentage of NZB/W mice if they are challenged with infectious pathogens or autoantigens [1]. Conversely, immune complex-mediated arthritis does develop in the transgenic K/BXN mouse model, in which the T cell has dual specificity for glucose-6-phosphate isomerase (GPI), presented by I-A^{g7} plus GPI epitopes 282–294 and another T-cell receptor-recognizing MHC A^{k} plus RNase 42–56 [2, 3]. K/BXN mice have not been shown to develop lupus-like disease. Finally, although mice of the MRL-*fas*^{lpr} strain can develop both spontaneous arthritis and lupus, this strain carries a mutation of the *fas* gene, and such mutations are uncommon in patients with autoimmune diseases [4].

The BXD2 strain is one of the first set of BXD recombinant inbred (RI) strains of mice that were generated originally by Dr Benjamin A. Taylor at the Jackson Laboratory (Bar Harbor, ME, USA) by inbreeding the intercross progeny of a cross between C57BL/6J and DBA/2J strains for more than 20 generations [5, 6]. During the course of a survey to discover genetic loci that influence T-cell senescence by using a set of 20 of the

BXD RI strains, we observed the development of comparatively severe spontaneous arthritis in the BXD2 strain. Subsequent observations indicated that the arthritis develops spontaneously in specific pathogen-free conditions. The adult mice exhibit splenomegaly, autoantibody production and renal disease, but lymphadenopathy is not a pronounced feature. Autoimmune disease features developed by the BXD2 mice segregate in F2 intercross progeny. Genetic linkage analysis by using BXD RI strains indicates that the quantitative trait loci (QTL) influencing the development of autoantibodies in BXD RI mice are located close to previously identified autoimmune susceptibility loci. These results are the first to indicate that BXD2 mice is a novel polygenic autoimmune mouse model that spontaneously develops both generalized autoimmune disease, including renal disease, and chronic erosive arthritis.

Animals and methods

Mice. Young (6-week-old) male and female C57BL/6J, DBA/2J, BXD2 and 19 other strains of BXD RI mice were purchased from The Jackson Laboratory (Bar Harbor, ME, USA), and were bred under the auspices of the Animal Resources Program at the University of Alabama at Birmingham (UAB). The F2 intercross progeny were generated by crossing (BXD2 × DBA/2J)F1 progeny and by crossing (BXD2 × C57BL/6J)F1 progeny. One hundred (BXD2 × D2) × (BXD2 × D2)F2 and 15 (BXD2 × B6) × (BXD2 × B6)F2 mice were generated to allow the segregation of the BXD2 lupus and arthritis loci and features. The evaluation and analysis was limited to female mice, unless otherwise specified. All mice were housed in a room equipped with an air-filtering system. The cages, bedding, water and food were sterilized, and the mice were handled with sterile gloves. All animal procedures performed were approved by The UAB Institutional Animal Care and Use Committee.

Evaluation of the development of arthritis and joint damage. A caliper was used in order to determine the thickness of each paw of each mouse. Paw swelling was determined as the increase in thickness, compared to the thickness at the initiation of the experiment. The severity of arthritis was graded according to the following scale: 0, normal with no swelling and erythema and no increase in joint diameter; 1, slight swelling and erythema with 0.1–0.3-mm increase in joint diameter; 2, swelling and erythema with 0.3–0.6-mm increase in joint diameter; 3, extensive swelling and erythema with 0.6–0.9-mm increase in joint diameter; 4, pronounced swelling and erythema with joint thickness of 0.9–1.2-mm visible joint deformity or ankylosis. Mice with a joint severity score of ≥ 1 in at least one limb are considered positive for arthritis.

After the mice were killed, the joints (hindlimb, forelimb, ankle and wrist) were harvested and were fixed in 10% formaldehyde/PBS for at least 24 h; they were decalcified by using EDTA for 4 weeks; they were paraffin-embedded and were sectioned at 5-μm thickness; then they were deparaffinized, and were stained with hematoxylin and eosin (H&E) (CMS, Houston, TX, USA).

Immunohistochemical analysis of tissue sections. For immunofluorescence studies, sections were cut into 4-μm slices, were placed on silanized slides, were washed in acetone 20 times and were then washed in water until they became clear. Slides were then washed in PBS, and fluorescent antibodies were applied at 150–200 μl per slide. FITC-conjugated goat anti-mouse immunoglobulin G (IgG) was purchased from ICN Biochemicals (Irvine, CA, USA) and was used at dilutions of 1:5 or 1:10. Slides were incubated with antibody in the dark at room temperature for 45 min and were then washed for 10 min in running water. Coverslips were applied with aqueous mounting medium, and the slides were stored at 4 °C. Staining was evaluated by using a fluorescence microscope (Vanox-T research microscope; Olympus, Tokyo, Japan).

For the analysis of the infiltration of B or T cells in the tissue, paraffin-embedded kidney sections (4-μM thickness) were analysed by means of immunohistochemistry with an anti-B220 or anti-CD3 antibody, as we have described previously [7, 8]. The quenching of endogenous peroxidase was performed by incubating tissue sections with 3% H_2O_2 at room temperature for 15 min in a humidified chamber. After washing with PBS, tissue sections were incubated with 0.25% pepsin at 37 °C for 30 min to reveal fixed antigen epitopes. Tissue sections were then treated with blocking solution at room temperature for 30 min followed by incubation at room temperature for 1 h with a biotin-conjugated rat anti-mouse B220 antibody (IgG_{2a} isotype) (eBioscience, San Diego, CA, USA) or a horseradish peroxidase (HRP)-conjugated anti-CD3 (DAKO, Carpinteria, CA, USA). An HRP-conjugated anti-rat IgG_{2a} antibody was used as the secondary antibody for B220 staining. The sections were then treated with the DAB staining kit (SK4100, Vector Laboratories, Burlingame, CA, USA) and were counterstained by means of incubation with methyl green at 65 °C for 3 min.

ELISA quantification of total Ig, autoantibodies to DNA, rheumatoid factor (RF) And urinary albumin. The concentration of the isotype-specific total Ig, anti-DNA antibodies or RF in the circulating blood was quantified by using an ELISA assay, as described previously [9]. Briefly, ELISA plates were coated with isotype-specific goat anti-mouse Ig antibodies (IgG1, IgG2a, IgG2b or IgM, 2 μg/ml each), 5 μg/ml of calf thymus dsDNA (Sigma-Aldrich, St Louis, MO, USA) or 1 μg/ml of affinity-purified rabbit IgG for the detection of total Ig, anti-DNA or RF, respectively, at 37 °C overnight. The plates were then washed with PBS–Tween-20 (PBS–T) and were blocked for 60 min with PBS–T plus 3% milk (PBS–T milk). Sera were diluted in PBS–T milk, were transferred to the plates

and were incubated for 45 min at room temperature. The assay was then performed, as described previously, with HRP-conjugated isotype-specific goat anti-mouse IgG or goat anti-mouse IgM (Southern Biotechnology Associates, Birmingham, AL, USA). Colour development was performed by using 3,3′,5,5′-tetramethylbenzidine as the substrate. The reaction was stopped by means of acidification and the plate was read at 450 nm by using an Emax Precision Microplate Reader (Molecular Device, Sunnyvale, CA, USA).

Albumin in urine was measured with the help of a competitive ELISA (Albuwell M, Exocell Inc., Philadelphia, PA, USA) according to the manufacturer's instructions. The levels of urinary albumin determined by means of this method were further compared with those measured with the help of the standard clinical determination of protein urinalysis by using the Albustix method (Bayer Corporation, Elkhard, IN, USA). Values obtained by using both methods exhibited a highly significant correlation ($P < 0.0001$).

Databases and genotype of BXD RI mice. The current mapping data files for BXD RI strains were generated by Williams *et al.* [10, 11] and Taylor *et al.* [5]. This data set can be downloaded at http://www.nervenet.org. All loci with redundant SDPs were purged, leaving a final BXD RI genotype marker set of approximately 620 unique non-redundant markers. A summary of information on chromosomal positions of the MIT microsatellite markers was obtained from the Portable Dictionary of the Mouse Genome (http://www.nervenet.org/fmpfiles/fmplist.html) [10] and the MIT Whitehead SSLP database (http://www.broad.mit.edu/cgi-bin/mouse/sts_info?database=mouserelease) [12]. Additional databases devoted to previously mapped QTL and polymorphic genes and markers between B6 and D2 strains of mice were obtained from the Mouse Genome Database (http://www.jax.org) [13, 14]. Relational database files between various phenotypes measured by using BXD RI strains of mice are available from the WebQTL (http://www.webqtl.org or http://www.genenetwork.org) [15, 16].

Statistics of genetic linkage analysis. Loci with log of the odds ratio (LOD) scores greater than approximately 2.8 ($P < 1.6 \times 10^{-3}$) and 4.3 ($P < 5.2 \times 10^{-5}$) were considered suggestive and significant, respectively [17]. Chromosomes (Chr) harbouring suggestive loci were analysed by means of simple interval mapping. Genomewide (experimentwise) significance probabilities for mapped QTL were estimated by comparing peak likelihood ratio statistics (LRS) ($\text{LRS} = \text{LOD} \times 4.6$) of correctly ordered data sets with those computed for >1000 permutations of the phenotype data [18]. Probabilities reported below as 'genomewide' (P_G) reflect the correction for multiple tests; other reported probabilities are comparisonwise. Confidence of QTL position is given as the 2-LOD support interval that locates the QTL within an approximate 95% confidence interval [19].

QTL analysis. The values were analysed by using the software program MapManager QTX (KF Manley, http://www.mapmanger.org) [20] and WebQTL (http://www.webqtl.org) [15, 16] in order to perform a genomewide search for mapping QTL. In this case, the user is not required to discriminate between 'B' and 'D' phenotypes. Rather, the quantitative phenotypic data for each RI strain serve as the starting point for analysis. This results in statistics that are essentially two-tailed, more conservative than may be warranted in some situations with extreme differences between parental lines. Irrespective of the complexity, the strategy for mapping is to detect the most similar, if not identical, SDPs from the large list of genotypes mapped in BXD strains. A concordance between a phenotypic SDP and an existing genotypic SDP (map location) indicates the presence of a QTL at or near that location contributing to the phenotype. However, owing to the limited number of BXD strains available, the number of SDPs to be compared, and consequently the complexity of testing required to establish concordance, a close match of SDPs may occur by chance [18]. As with all statistical comparisons, it is necessary to make a calculation of the probability that the observed result is a false positive. We, therefore, have calculated the genomewide probability of obtaining the observed linkages by random chance corresponding to an error threshold of $P = 0.05$, that is, one chance in 20 of such a false-positive error. We performed this by using a non-parametric permutation method developed by Churchill and Doerge [18], which is implemented in the Map Manager QTX software [20] and WebQTL program (http://www.webqtl.org or http://www.genenetwork.org) [15, 16].

A subroutine of the Map Manager QTX software [20] and WebQTL [15, 16] by using computationally efficient regression equations has been used for mapping the QTL. The probability of linkage between our traits and previously mapped genotypes was estimated at 1-cM intervals along the entire genome, except for the Y Chr. The statistical power of linkage of the phenotype to individual genotypes (pointwise linkage statistics) that attained values between 0.0001 and 0.00002 was considered to have reached a level of genomewide statistical significance. Linkages approximating that level are deemed 'suggestive' and are worthy of reporting, although confirmation of linkage is required [18]. In order to establish criteria for suggestive and significant linkage, a permutation test is performed by using Map Manager QTX (>1000 permutations at 1-cM intervals) [18]. This test compares the peak LRS score obtained for a given data set with the peak LRS score obtained for 1000 random permutations of the same data set. The latest iteration of Map Manager allowed us to apply a weighted least-square regression model, which resulted in a greater power and precision in mapping QTL.

Statistical analysis. The results are expressed as the mean ± SD of the mean (SEM). The two-tailed Student's

t-test was used for statistical analysis. A one-way analysis of variance was used when more than two groups of samples were compared. Correlations between various variables were determined by using a linear regression analysis. A *P*-value of <0.05 was considered significant.

Results

Spontaneous erosive arthritis in BXD2 mice

The development of spontaneous erosive arthritis in BXD2 mice has not been reported previously, probably because it is most obvious in older mice. This was observed because of the severity of the irreversible joint deformity in BXD2 mice during an ageing study of T-cell senescence in BXD RI strains of mice (Fig. 1A). We followed at least 19 strains of BXD RI mice to 24 months of age for the thymic involution studies, and observed that none of the other BXD RI strains of mice developed arthritis.

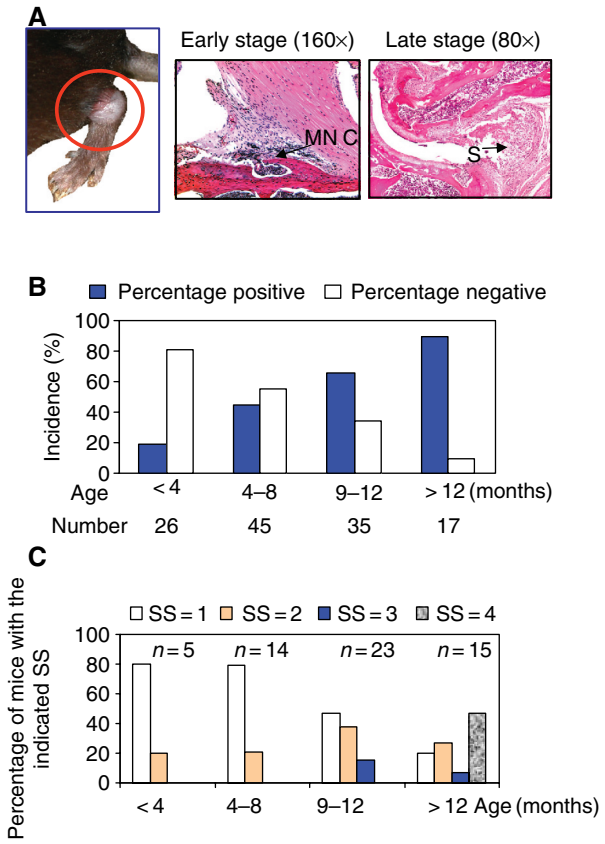

Figure 1 Arthritis in BXD2 mice. (A) Illustration of typical arthritis in the ankle or knee joint of a 12-month-old BXD2 female mouse. H&E staining of the joint lesion in a representative BXD2 mouse. (B) The incidence of arthritis in female BXD2 mice ($n=123$ total, $P<0.0001$, χ^2-test for trend). (C) The severity of arthritis in BXD2 mice with arthritis at various ages. Arthritis was defined to be present if at least one joint exhibited slight swelling, erythema and increased joint diameter. Joint severity has been defined in the section entitled 'Materials and methods'. MNC, mononuclear cell infiltration; S, synovial hyperplasia; SS, severity score.

Histopathologic evaluation of the musculoskeletal system showed the development of synovitis and arthritis in adult BXD2 mice that exhibit histologic similarities to RA in humans, including extensive synovial hyperplasia and marginal invasion, affecting the small metatarsophalangeal joints as well as the larger (forelimb and hindlimb) joints (Fig. 1A). The early-stage arthritis is characterized by an acute to subacute inflammatory synovitis. The late-stage arthritis is characterized by synovial cell hyperplasia, pannus formation and severe erosion of cartilage underlying bone (Fig. 1A). The arthritis affects 50% of female mice by 8 months and 90% at ages >12 months (Fig. 1B). The severity (Fig. 1C) of arthritis in the affected female BXD2 mice has been scored according to the age of the mice. The results show a progressive age-related increase in the severity of arthritis. Intriguingly, arthritis was observed in both male and female mice; however, the incidence of arthritis in female mice is higher than that in male mice (66 versus 42% between 9 and 12 months of age; $n=35$ and 21, respectively).

Development of glomerulonephritis (GN) and generalized autoimmune disease in the BXD2 mice

The lifespan of BXD2 mice has been reported as being 14 months [21], which is one of the shortest among the 21 strains of BXD RI mice that were examined [21]. We, therefore, determined whether the development of autoimmune pathologic features can be identified from tissue sections of BXD2 mice. Diffuse proliferative GN was observed consisting of inflammatory cell infiltration into the glomeruli leading to mesangial proliferation and later glomerular atrophy. The GN consists of increased cellularity (Fig. 2A), infiltration of $B220^+$ B cells and $CD3^+$ T cells surrounding the capillaries and mesangial cells of glomeruli (Fig. 2B), and immune complex deposition in the glomeruli (Fig. 2C). Significant increased proteinuria develops by 6 months (Fig. 2D). BXD2 mice exhibit pathogenic characteristic of clinical arthritis and lupus, including spontaneous inflammation and progressive destruction of the joints and the kidney. These mice can thus be used in order to segregate the pathogenic mechanisms associated with the development of lupus and arthritis.

Development of lupus and/or arthritis in F2 mice

In order to determine whether the development of generalized autoimmune disease and arthritis in BXD2 mice is caused by a single mutation or a complex mixture of genetic effects, we generated 115 F2 mice by crossing (BXD2 × DBA/2J)F1 progeny and by crossing (BXD2 × C57BL/6J)F1 progeny. All F2 mice (both females and males) were killed between 10 and 12 months of age and urinary albumin was plotted against joint score (Fig. 3). Among the F2 mice, 6.1% developed only arthritis, 20.1% developed only increased

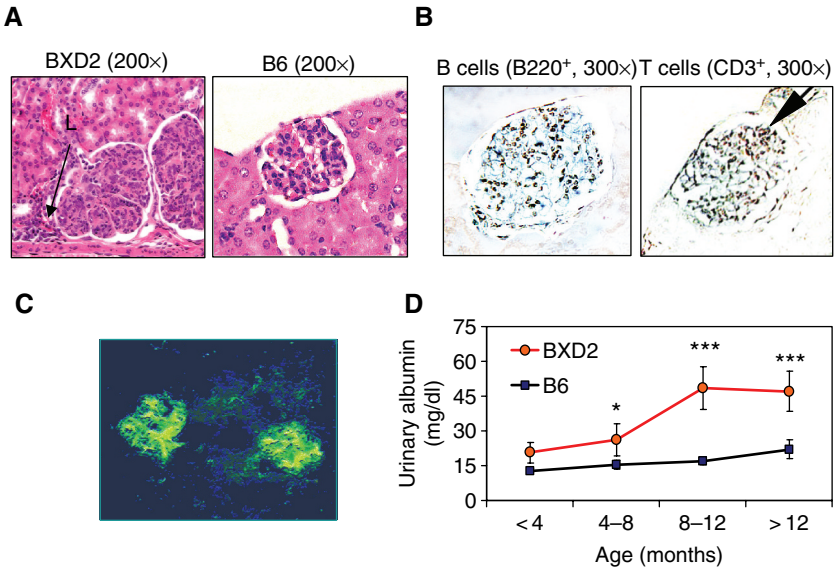

Figure 2 Renal disease and T- and B-cell infiltration in BXD2 mice. (A) H&E staining of the kidney of a representative 13-month-old BXD2 mouse and a B6 mouse. (B) Immunohistochemical staining of a B220- or a CD3-positive lymphocytes in the glomerulus (arrow indicated) from an 8-month-old BXD2 mouse. (C) Immunohistochemical analysis of immunecomplexes in the glomeruli of a representative BXD2 mouse by using FITC-conjugated goat anti-mouse immunoglobulin G (IgG). (D) Urinary albumin (mean ± SEM) in BXD2 or B6 female mice at various ages (5–8 mice/group; $^{*}P < 0.05$ and $^{***}P < 0.001$ between the same age group). L, lymphocytic infiltrate.

urinary albumin, 6.1% developed both arthritis and increased urinary albumin and 67.8% did not develop increased urinary albumin or arthritis. These results suggest that the effects of several genes contribute to autoimmune disease, which can be specific for predisposing to the development of either lupus or arthritis in BXD2 mice.

Development of both lupus- and arthritis-related autoantibodies in BXD2 mice

We then determined whether BXD2 mice exhibited polyclonal B-cell activation and developed sera containing high-affinity autoantibodies related to both lupus and arthritis. There was a significant age-related increase in serum titers of IgG1 and IgG2b total Ig in BXD2 mice (Fig. 4). High levels of antibodies against DNA and RF are produced in BXD2 mice at 6 months of age, with the predominant isotypes being IgG1 and IgG2b (Fig. 4).

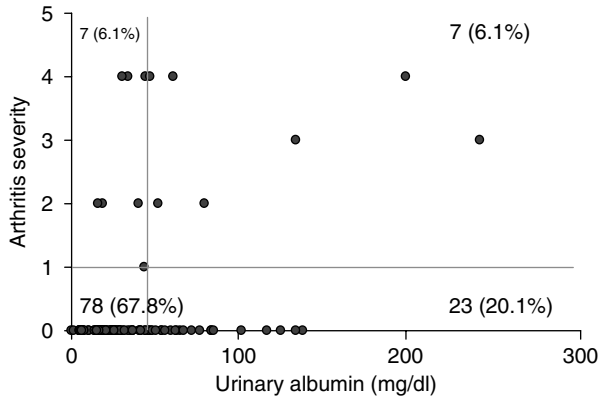

Figure 3 Segregation of lupus and arthritis in F2 mice. F2 mice were generated by brother × sister mating of the (BXD2 × DBA/2)F1 or (BXD2 × B6)F1 mice. The development of lupus and arthritis was determined in 100 (BXD2 × DBA/2) × (BXD2 × DBA/2)F2 and 15 (BXD2 × B6) × (BXD2 × B6)F2 mice between 10 and 12 months of age. Urinary albumin and arthritis were determined, as described in the section entitled 'Materials and methods'. The cut-off lines were determined as the level of urinary albumin (the vertical line) or arthritis score (the horizontal line) greater than mean ± SEM from the 115 F2 mice.

Serum titres of autoantibodies against DNA and RF were then determined in BXD2 as well as 19 other strains of BXD RI mice. At 13 months of age, BXD2 mice exhibited the highest serum titers of all isotypes (IgG1, IgG2a, IgG2b and IgM) anti-DNA (Fig. 5). High levels of IgG2a anti-DNA were observed in BXD6, BXD9 and BXD18, whereas high levels of IgG2b anti-DNA, the isotype most characteristic of BXD2 strain, were observed also in BXD1 and, to a lesser extent, in BXD20. The total anti-DNA was significantly correlated with the IgG-specific ($r^2 = 0.96$, $P < 0.0001$) and the IgM-specific anti-DNA ($r^2 = 0.67$, $P < 0.0001$), and thus the total anti-DNA was used as a quantitative trait for the genetic linkage analysis.

Similar to anti-DNA, the highest levels of IgG2b RF were also seen in autoimmune BXD2 mice (Fig. 6). High levels of IgG2b RF were observed in 13-month-old BXD1, 11, 25, 29 and parental B6 (Fig. 6). Intermediate (>400) levels of IgG2a RF were seen in BXD strains BXD12, BXD15 and BXD24, and intermediate (>400) levels of IgG1 RF were seen in BXD strains BXD6, BXD9, BXD15, BXD30 and BXD32, as well as in parental D2. Certain strains, such as BXD14, BXD16, BXD19, BXD20, BXD22, BXD25 and BXD28 did not produce significant levels of RF of any isotypes.

Genetic linkage analysis of autoantibodies in BXD RI mice

The BXD RI strain set was developed for the purpose of genetic linkage analysis [22]. Because the production

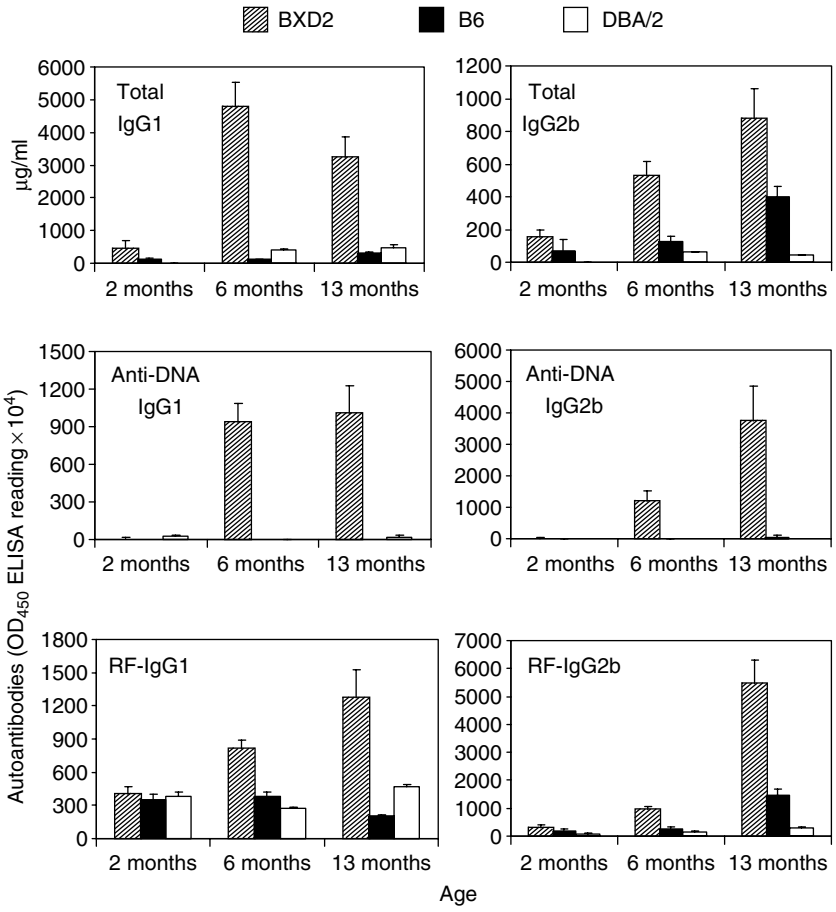

Figure 4 Age-dependent increase in serum titers of total immunoglobulin (Ig), anti-DNA and rheumatoid factor (RF). Serum titers of IgG1 and IgG2b total Ig, and IgG1 and IgG2b isotype-specific anti-DNA and RF in control B6, DBA/2 and autoimmune BXD2 mice at the indicated age were determined by using an ELISA method. The results represent mean ± SEM of three to four mice/group.

of high-affinity autoantibodies is a pronounced autoimmune feature in BXD2 mice and no other BXD RI strains develop overt features of arthritis, we used the total serum levels of anti-DNA and RF measured in 13-month-old mice of the BXD RI strains as the primary trait (data from Figs 5 and 6) in order to map the putative QTL that may be associated with the development of autoantibodies in the BXD2 strains of mice. The QTL near Chr 2 (*D2Mit412*) has been shown to be close to the renal disease susceptibility locus in the (New Zealand Black- × New Zealand White)F1 hybrid mouse model of systemic lupus erythematosus (Fig. 7A and Table 1) [23]. The QTL located on mouse Chr 4 (53.6 cM, identified by the *D4Mit146* marker) is close to the autoimmune susceptibility or suppressor *Sle2, Lbw2, Lmb1, Sles2, Nba1* and *Asm2* loci that have been identified previously in mice with the NZM2410, NZB × NZW, B6, MRL and MRL-lpr background (Fig. 7A and Table 1) [1, 24–32].

Significantly elevated serum titers of anti-DNA were observed in BXD RI strains with a D allele at the *D2Mit412* versus those with a B allele at the same locus (5.77 ± 0.43 versus 1.98 ± 0.67, $P < 0.0001$) (Fig. 7B). Thus, the presence of the B allele at *D2Mit412* confers a suppressive effect for the production of anti-DNA. In BXD strains BXD14, BXD16, BXD19, BXD22 and BXD28, there were undetectable levels of anti-DNA. With the exception of BXD27 and D2, all strains (BXD1, BXD2, BXD6, BXD9, BXD12, BXD18, BXD20, BXD25, BXD30 and BXD32) that carried a D allele at *D2Mit412* produced high levels of anti-DNA (Fig. 7B, upper panel).

Similarly, a significantly elevated serum titers of RF was observed in BXD RI strains with a B allele at the *D4Mit146* versus those with a D allele at the same locus (6.66 ± 0.11 versus 7.79 ± 0.37, $P = 0.0007$). With the exception of BXD20, all strains (BXD2, BXD11, BXD24 and BXDB6) that carry a B allele at *D4Mit146* produced high levels of RF (Fig. 7B, lower panel). These results indicate that the presence of a D allele on Chr 2 and a B allele on Chr 4 is associated with a high anti-DNA and RF response, respectively, in BXD RI strains of mice.

Discussion

Several autoimmune loci (*Lbw*, *Sle*, Sle suppressor (*Sles*), *Lmb and Asm2*) associated with the development of generalized autoimmune disease in NZB/W, NZM2410 and (MRL-Fas^{lpr} × B6-Fas^{lpr})F_2 (abbreviated as MBF2), or MRL-lpr mice, have been genetically mapped [30–38]. These models primarily exhibit a B-cell defect, with an accompanying T-cell defect, and the mice exhibit

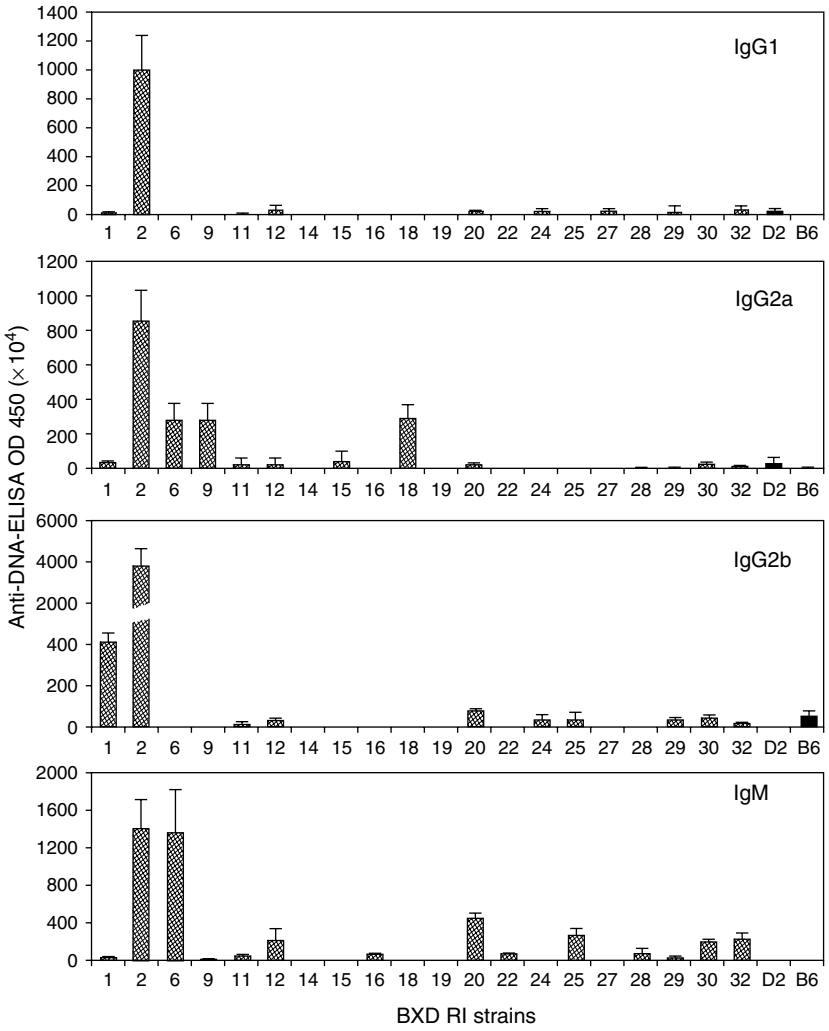

Figure 5 Serum titres of anti-DNA in BXD recombinant inbred (RI) strains of mice. Serum levels of isotype-specific anti-DNA antibodies in 13-month-old B6, DBA/2, BXD2 and 19 other BXD RI strains of mice were determined by using an ELISA method. The results represent mean ± SEM of three to four mice/group.

elevated levels of serum Ig, autoantibodies and immunecomplex-mediated autoimmune disease [39–41]. Genetic linkage analysis clearly shows that the development of these features is inherited as a polygenic trait. Certain genetic loci, such as *Sle1, Sle2, Sle3* and *Sle5*, exhibited dual or multiple effects in order to influence the development of GN, the production of anti-nuclear autoantibodies, splenomegaly and polyclonal T- and B-cell hyperactivities. By contrast, certain genetic loci, such as *Sle4* and *Sle6*, only exhibit a single effect on one autoimmune trait. Furthermore, despite the differences between the NZB/W, B6 and MRL genetic background, common loci, such as *Lmb1, Lbw2, Asm2* and *Sles2*, have been identified to influence the generalized autoimmune phenotype, suggesting that these loci harbour critical genes that exhibit strong effects on the susceptibility or suppressive effects on generalized autoimmune disease.

The present results indicate that in BXD2 mice there is spontaneous production of autoantibodies, as well as erosive arthritis and diffuse GN, at adult age. These mice, however, do not die at a very young age as do arthritis-susceptible motheaten (*me/me*) mice that carry a single mutation of the *Hcph* gene [9, 42]. Unlike BXSB mice, the disease occurs in both female and male mice, although predominately in female mice, and is not associated with the Y Chr accelerator gene [43]. Mozes *et al.* [44] have previously shown that, among the 15 strains of BXD RI strains included in their study, the BXD2 strain of mice produced the highest serum titers of anti-ssDNA antibody after immunization with the human monoclonal anti-DNA antibody expressing the 16/6Id idiotype. The results of our study indicate that the BXD2 strain spontaneously develops age-related increased serum titers of total IgG1 and IgG2b, suggesting that polyclonal B-cell activation is an abnormal immune feature in BXD2 mice.

The incidence and severity in specific pathogen-free BXD2 RI mice have now been monitored over 3 years. Because no differences have been observed among the groups of mice housed in specific pathogen-free mouse rooms located in three buildings, pathogenic microbial organisms do not contribute to the development of arthritis

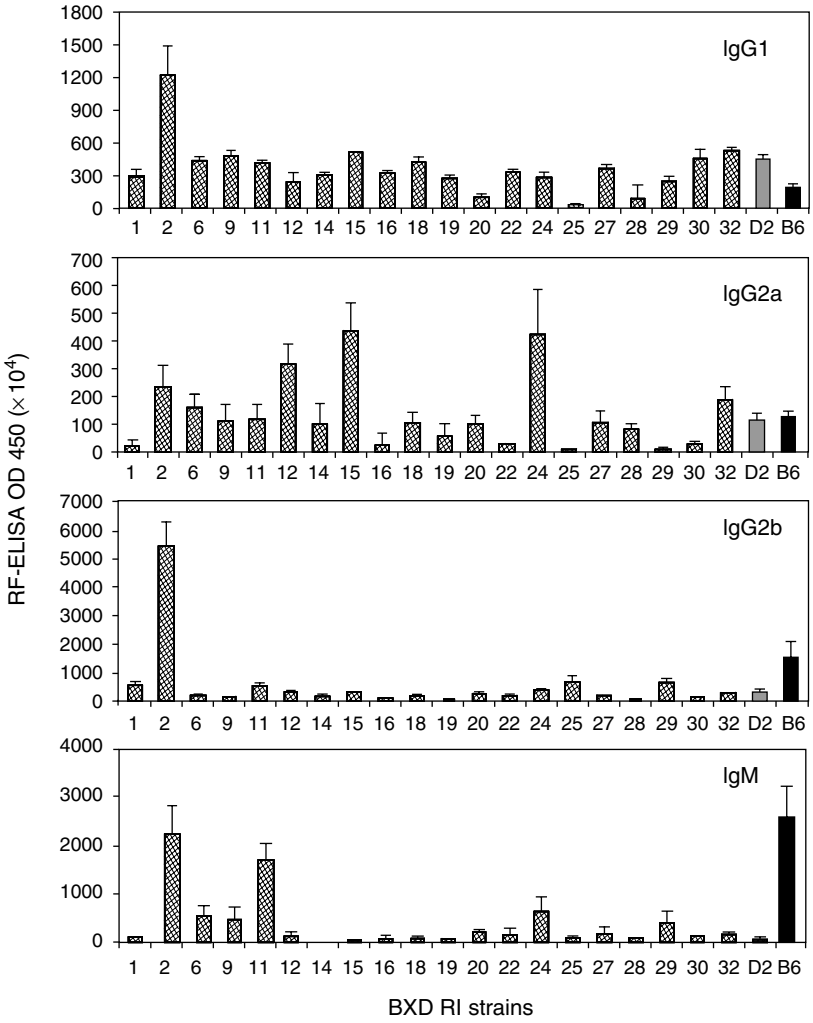

Figure 6 Serum titers of rheumatoid factor (RF) in BXD recombinant inbred (RI) strains of mice. Serum levels of isotype-specific RF in 13-month-old B6, DBA/2, BXD2 and 19 other BXD RI strains of mice were determined by using an ELISA method. The results represent mean ± SEM of three to four mice/group.

in the BXD2 mice. The parental strains are the commonly used B6 and DBA/2 inbred strains and these strains do not develop either lupus or arthritis. The serum titers of IgM, IgG1 and IgG2a and IgG2b anti-DNA antibodies are low in young and aged B6 and DBA/2 parental strains (Figs 4 and 5). Similarly, the serum titers of IgG1 and IgG2a RF are low in young and aged B6 and DBA/2 parental strains (Figs 4 and 6). There were higher titers of IgG2b and IgM RF in 13-month-old B6 mice, compared to those in DBA/2 mice (Fig. 6). This is consistent with the genetic linkage analysis, showing that a B allele at *D4Mit146* is associated with increased serum titers of RF in BXD RI strains of mice (Fig. 7).

The findings of our study document the presence of an RF susceptibility locus (Chr 4, 54 cM) contributed by the B6 allele. This is consistent with the previous results reported by Vidal *et al.* [1] who showed the presence of a lupus susceptibility locus (*Lmb1*) in the normal B6 background, whose contribution appeared equal to the other MRL-derived lupus susceptibility QTL. There are seven additional autoimmune SLE susceptibility, SLE suppressor and sialadenitis susceptibility loci previously mapped at the vicinity of the Chr 4 locus identified in the present study (Table 1) [1, 24–32]. The *D2Mit412* locus mapped for anti-DNA in the present study also matched with the previously mapped genetic loci predisposing mice to GN, anti-DNA antibodies and renal disease (Table 1) [23]. The results of our study, therefore, support previous findings and indicate that there is considerable genetic heterogeneity for lupus and arthritis susceptibility genes that involve even the commonly used normal strains of mice. The F2 experiment further suggests that the features of lupus and arthritis developed by the BXD2 mice can be segregated and that they are highly specific to the genotype of the BXD2 strain. This suggests that there are multiple independent interacting loci, consisting of various genes contributed by the C57BL/6 strain or the DBA/2 strain that are required for these autoimmune traits to be manifest. This is consistent with our preliminary F2 linkage analysis of proteinuria, anti-DNA and RF, which indicates the presence of at least five significant QTL for these traits on various Chr (Hsu *et al.*, unpublished

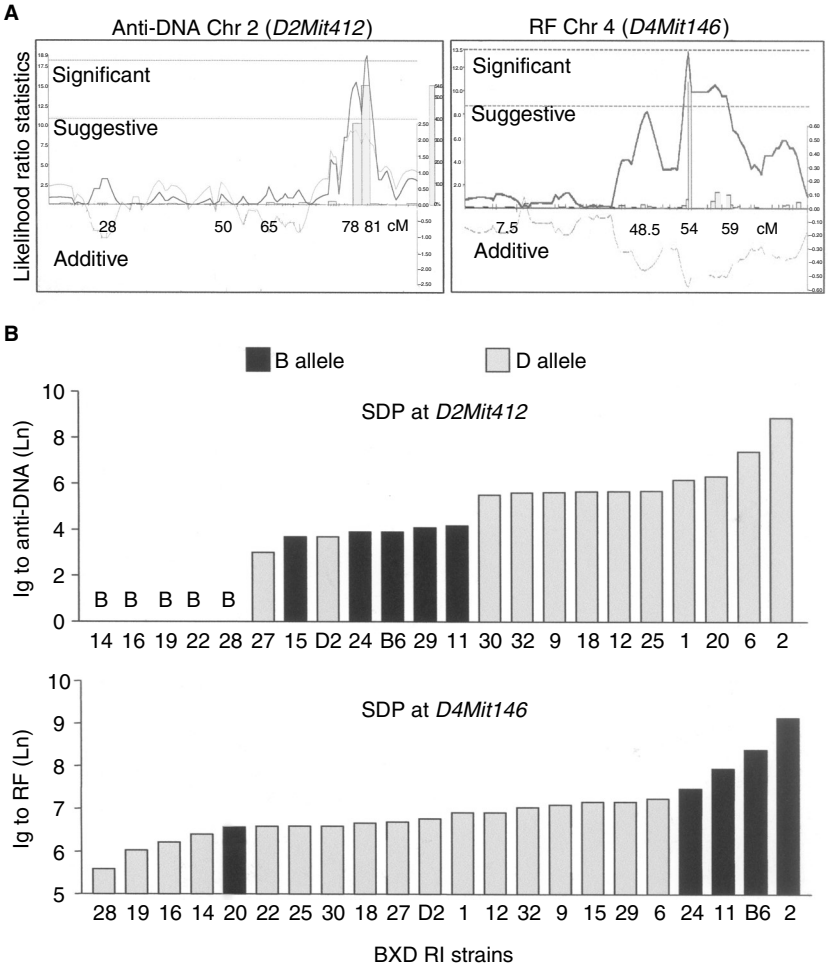

Figure 7 Genetic linkage analysis of anti-DNA and rheumatoid factor (RF) in 13-month-old BXD recombinant inbred (RI) strains of mice. (A) Quantitative trait loci (QTL) associated with anti-DNA and RF in 13-month-old BXD RI strains of mice were mapped by using WebQTL and including B6 and D2 in the mapping analysis. The likelihood ratio statistics (LRS) plot shows the results of the interval mapping of anti-DNA and RF at mouse *D2Mit412* (left panel; WebQTL ID 10697) and *D4Mit146* (right panel; WebQTL ID 10698), respectively. The dark grey line is the LRS value and the light grey line is an estimate of the additive effects of substituting a single B allele for D allele in the test interval. A permutation test was performed in order to establish criteria for suggestive and significant linkage. (B) Comparison of genotype and phenotype of *D2Mit412 and D4Mit146*. The allele distribution of each BXD RI strain at the mapped locus was downloaded from http://www.nervenet.org. Each bar graph represents the average of either anti-DNA or RF from a BXD RI strain of mice.

observations). The results of our study, thus, strongly indicate that the autoimmune disease development in BXD2 mice is caused by complex interactions of multiple genes inherited from the original parental B6 and DBA/2 mice. Thus, the BXD2 mouse is a novel polygenic spontaneous autoimmune mouse that can be used for studying the genetic and cellular basis of multiple autoimmune diseases, including lupus nephritis and erosive arthritis.

Table 1 Quantitative trait loci (QTL) influencing the production of anti-DNA and rheumatoid factor (RF) in 13-month-old BXD recombinant inbred (RI) strains of mice

Marker	LRS	Chr	cM	Dominant allele	Other QTL	cM	Phenotype
Anti-DNA							
D2Mit412	18.9	2	78	D	*Rends**	86	Renal disease susceptibility
D2Mit51	14.6	2	81	D	*Rends*	86	Renal disease susceptibility
RF							
D4Mit146	10	4	53.5	B	*Adaz1*	50	Anti-dsDNA production
					Arvm2	58	Autoimmune renal vasculitis
					Asm2	53.6	Sialadenitis in MRL/lpr
					Im2	55	Immunoregulatory 2
					Lbw2	55	Lupus in (NZB × NZW)F2
					Lmb1	58	Lupus in MRL-Fas^{lpr} and B6-Fas^{lpr} F2 mice
					Sles2	58	SLE suppressor 2
					Spm1	49	Splenomegaly modifier

*The QTL of previously mapped genetic loci associated with lupus and autoimmune disease features were obtained from the database of Mouse Genome Informatics website maintained by the Jackson Laboratory (http://www.informatics.jax.org/).

Acknowledgments

This work was supported by NIH grants RO1 AG11643, RO1 AG 16653, a UAB HSF-GEF grant, a Birmingham VAMC Merit Review Grant and a research grant from Sankyo Pharmaceutical Inc., Ltd. HCH is a recipient of the Arthritis Foundation Arthritis Investigator Award. The authors thank Dr Fiona Hunter for expert review of the manuscript, and Ms. Carol Humber for excellent secretarial assistance.

References

1 Vidal S, Kono DH, Theofilopoulos AN. Loci predisposing to autoimmunity in MRL-Fas lpr and C57BL/6-Faslpr mice. J Clin Invest 1998;101:696–702.
2 Basu D, Horvath S, O'Mara L, Donermeyer D, Allen PM. Two MHC surface amino acid differences distinguish foreign peptide recognition from autoantigen specificity. J Immunol 2001;166: 4005–11.
3 Schaller M, Burton DR, Ditzel HJ. Autoantibodies to GPI in rheumatoid arthritis: linkage between an animal model and human disease. Nat Immunol 2001;2:746–53.
4 Watanabe-Fukunaga R, Brannan CI, Copeland NG, Jenkins NA, Nagata S. Lymphoproliferation disorder in mice explained by defects in Fas antigen that mediates apoptosis. Nature 1992;356: 314–7.
5 Taylor BA, Wnek C, Kotlus BS, Roemer N, MacTaggart T, Phillips SJ. Genotyping new BXD recombinant inbred mouse strains and comparison of BXD and consensus maps. Mamm Genome 1999;10:335–48.
6 Morse HC III, Chused TM, Hartley JW, Mathieson BJ, Sharrow SO, Taylor BA. Expression of xenotropic murine leukemia viruses as cell-surface gp70 in genetic crosses between strains DBA/2 and C57BL/6. J Exp Med 1979;149:1183–96.
7 Hsu HC, Zhang HG, Song GG *et al.* Defective Fas ligand-mediated apoptosis predisposes to development of a chronic erosive arthritis subsequent to *Mycoplasma pulmonis* infection. Arthritis Rheum 2001;44:2146–59.
8 Liu Z, Xu X, Hsu HC *et al.* CII-DC-AdTRAIL cell gene therapy inhibits infiltration of CII-reactive T cells and CII-induced arthritis. J Clin Invest 2003;112:1332–41.
9 Su X, Zhou T, Yang P, Edwards CK III, Mountz JD. Reduction of arthritis and pneumonitis in motheaten mice by soluble tumor necrosis factor receptor. Arthritis Rheum 1998;41:139–49.
10 Williams RW, Gu J, Qi S, Lu L. The genetic structure of recombinant inbred mice: high-resolution consensus maps for complex trait analysis. Genome Biol 2001;2:RESEARCH0046.
11 Airey DC, Lu L, Williams RW. Genetic control of the mouse cerebellum: identification of quantitative trait loci modulating size and architecture. J Neurosci 2001;21:5099–109.
12 Dietrich W, Katz H, Lincoln SE *et al.* A genetic map of the mouse suitable for typing intraspecific crosses. Genetics 1992;131:423–47.
13 Blake JA, Richardson JE, Bult CJ, Kadin JA, Eppig JT. MGD: the mouse genome database. Nucleic Acids Res 2003;31:193–5.
14 Blake JA, Richardson JE, Davisson MT, Eppig JT. The mouse genome database (MGD): genetic and genomic information about the laboratory mouse. The Mouse Genome Database Group. Nucleic Acids Res 1999;27:95–8.
15 Wang J, Williams RW, Manly KF. WebQTL: web-based complex trait analysis. Neuroinformatics 2003;1:299–308.
16 Chesler EJ, Lu L, Wang J, Williams RW, Manly KF. WebQTL: rapid exploratory analysis of gene expression and genetic networks for brain and behavior. Nat Neurosci 2004;7:485–6.
17 Lander E, Kruglyak L. Genetic dissection of complex traits: guidelines for interpreting and reporting linkage results. Nat Genet 1995;11:241–7.
18 Churchill GA, Doerge RW. Empirical threshold values for quantitative trait mapping. Genetics 1994;138:963–71.
19 Lynch M, Walsh B. Genetics and Analysis of Quantitative Traits. Sunderland, MA: Sinauer, 1998.
20 Manly KF, Cudmore RH Jr, Meer JM. Map Manager QTX, cross-platform software for genetic mapping. Mamm Genome 2001;12: 930–2.
21 Gelman R, Watson A, Bronson R, Yunis E. Murine chromosomal regions correlated with longevity. Genetics 1988;118:693–704.
22 Peirce JL, Lu L, Gu J, Silver LM, Williams RW. A new set of BXD recombinant inbred lines from advanced intercross populations in mice. BMC Genet 2004;5:7.
23 Rahman ZS, Tin SK, Buenaventura PN *et al.* A novel susceptibility locus on chromosome 2 in the (New Zealand Black × New Zealand White) F1 hybrid mouse model of systemic lupus erythematosus. J Immunol 2002;168:3042–9.
24 Kono DH, Burlingame RW, Owens DG *et al.* Lupus susceptibility loci in New Zealand mice. Proc Natl Acad Sci USA 1994;91:10168–72.
25 Ochiai K, Ozaki S, Tanino A *et al.* Genetic regulation of anti-erythrocyte autoantibodies and splenomegaly in autoimmune hemolytic anemia-prone New Zealand black mice. Int Immunol 2000;12:1–8.
26 Theofilopoulos AN, Kono DH. The genes of systemic autoimmunity. Proc Assoc Am Physicians 1999;111:228–40.
27 Morel L, Blenman KR, Croker BP, Wakeland EK. The major murine systemic lupus erythematosus susceptibility locus, *Sle1*, is a cluster of functionally related genes. Proc Natl Acad Sci USA 2001;98:1787–92.
28 Rozzo SJ, Vyse TJ, Drake CG, Kotzin BL. Effect of genetic background on the contribution of New Zealand black loci to autoimmune lupus nephritis. Proc Natl Acad Sci USA 1996;93:15164–8.
29 Morel L, Wakeland EK. Lessons from the NZM2410 model and related strains. Int Rev Immunol 2000;19:423–46.
30 Morel L, Croker BP, Blenman KR *et al.* Genetic reconstitution of systemic lupus erythematosus immunopathology with polycongenic murine strains. Proc Natl Acad Sci USA 2000;97:6670–5.
31 Johansson AC, Nakken B, Sundler M *et al.* The genetic control of sialadenitis versus arthritis in a NOD.Q×B10Q F2 cross. Eur J Immunol 2002;32:243–50.
32 Nishihara M, Terada M, Kamogawa J *et al.* Genetic basis of autoimmune sialadenitis in MRL/lpr lupus-prone mice: additive and hierarchical properties of polygenic inheritance. Arthritis Rheum 1999;42:2616–23.
33 Morel L, Rudofsky UH, Longmate JA, Schiffenbauer J, Wakeland EK. Polygenic control of susceptibility to murine systemic lupus erythematosus. Immunity 1994;1:219–29.
34 Wakeland EK, Morel L, Mohan C, Yui M. Genetic dissection of lupus nephritis in murine models of SLE. J Clin Immunol 1997;17:272–81.
35 Sobel ES, Morel L, Baert R, Mohan C, Schiffenbauer J, Wakeland EK. Genetic dissection of systemic lupus erythematosus pathogenesis: evidence for functional expression of Sle3/5 by non-T cells. J Immunol 2002;169:4025–32.
36 Talal N, Pillarisetty R, Papoian R, Roubinian J. Experimental lupus: a disorder of immunologic regulation. Adv Nephrol Necker Hosp 1976;6:37–45.
37 Theofilopoulos AN, Kono DH. A genetic analysis of lupus. Allergy 2002;57:67–74.
38 Theofilopoulos AN. Genetics of systemic autoimmunity. J Autoimmun 1996;9:207–10.
39 Theofilopoulos AN, Singer PA, Kofler R, Kono DH, Duchosal MA, Balderas RS. B and T cell antigen receptor repertoires in lupus/arthritis murine models. Springer Semin Immunopathol 1989;11: 335–68.

40 Theofilopoulos AN, McConahey PJ, Izui S, Eisenberg RA, Pereira AB, Creighton WD. A comparative immunologic analysis of several murine strains with autoimmune manifestations. Clin Immunol Immunopathol 1980;15:258–78.
41 Morel L, Mohan C, Yu Y *et al.* Multiplex inheritance of component phenotypes in a murine model of lupus. Mamm Genome 1999;10: 176–81.
42 Senecal JL, Rauch J, Grodzicky T *et al.* Strong association of autoantibodies to human nuclear lamin B1 with lupus anticoagulant antibodies in systemic lupus erythematosus. Arthritis Rheum 1999;42:1347–53.
43 Murphy ED, Roths JB. A Y chromosome associated factor in strain BXSB producing accelerated autoimmunity and lymphoproliferation. Arthritis Rheum 1979;22:1188–94.
44 Mozes E, Alling D, Miller MW *et al.* Genetic analysis of experimentally induced lupus in mice. Clin Immunol Immunopathol 1997;85:28–34.